Eur Biophys J (1998) 27: 490–500

ARTICLE

Denis Chrétien · Henrik Flyvbjerg · Stephen D. Fuller

Limited flexibility of the inter-protofilament bonds in microtubules assembled from pure tubulin

Received: 22 December 1997 / Revised version: 11 March 1998 / Accepted: 17 March 1998

Abstract The superposition of the regular arrangement of tubulin subunits in microtubules gives rise to moiré patterns in cryo-electron micrographs. The moiré period can be predicted from the dimensions of the tubulin subunits and their arrangement in the surface lattice. Although the average experimental moiré period is usually in good agreement with the theoretical one, there is variation both within and between microtubules. In this study, we addressed the origin of this variability. We examined different possibilities, including artefacts induced by the preparation of the vitrified samples, and variations of the parameters that describe the microtubule surface lattice. We show that neither flattening nor bending of the microtubules, nor changes in the subunit dimensions, can account for the moiré period variations observed in 12 and 14 protofilament microtubules. These can be interpreted as slight variations, in the range –0.5 Å to +0.9 Å, of the lateral interactions between tubulin subunits in adjacent protofilaments. These results indicate that the inter-protofilament bonds are precisely maintained in microtubules assembled in vitro from pure tubulin. The fact that the moiré period is not affected by bending indicates that the local interactions between tubulin subunits are sufficiently stiff to accommodate large deformations of the microtubule wall.

Key words Microtubule structure · Microtubule dynamics · Inter-protofilament bonds · Cryo-electron microscopy · Moiré patterns

Abbreviations *Cryo-EM* Cryo-electron microscopy · *CTF* Contrast transfer function · *MAPs* Microtubule associated proteins

D. Chrétien (✉)
Cell Biology, Cell Biophysics and Structural Biology Programmes,
European Molecular Biology Laboratory,
Meyerhofstrasse 1, Postfach 10 22 09,
D-69017 Heidelberg, Germany
e-mail: chretien@embl-heidelberg.de

H. Flyvbjerg
Condensed Matter Physics and Chemistry Department,
Risø National Laboratory,
DK-4000 Roskilde, Denmark
e-mail: henrik.flyvbjerg@risoe.dk

H. Flyvbjerg
The Niels Bohr Institute,
Blegdamsvej 17, DK-2100 Copenhagen Ø, Denmark
e-mail: henrik.flyvbjerg@nbi.dk

S. D. Fuller
Structural Biology Programme,
European Molecular Biology Laboratory,
Meyerhofstrasse 1, Postfach 10 22 09,
D-69017 Heidelberg, Germany
e-mail: fuller@embl-heidelberg.de

Introduction

Microtubules are built from the tubulin molecule which comprises two subunits (α, β) of comparable dimensions (Mr ~ 55,000 each, see Fig. 1a). They are involved in various functions including cell compartmentalization, organelle movement, cell division and cell motility (Hyams and Lloyds 1994). Unless they are stabilized by cellular factors, microtubules are dynamic polymers that alternate stochastically between growth and shrinking states (Mitchison and Kirschner 1984; Walker et al. 1988). Dynamic instability is finely regulated during the cell cycle by microtubule associated proteins (MAPs) through cascades of phosphorylation-dephosphorylation events (Hyman and Karsenti 1996). Owing to their fundamental role during mitosis, microtubules are a target for anti-mitotic drugs that interfere with microtubule dynamics, such as taxol and its derivatives (Avila 1990). Dynamic instability is built during microtubule assembly through the hydrolysis of the GTP bound to the β-subunit of the tubulin molecule (Caplow 1992; Erickson and O'Brien 1992). GTP-hydrolysis is thought to weaken the lateral interactions between protofilaments, resulting in an intrinsically unstable microtubule lattice. Conversely, MAPs or taxol are thought to stabilize microtubules by reinforcing these lateral interactions. Thus, it would be useful to have a method that allows direct visualization of the effect on the inter-protofil-

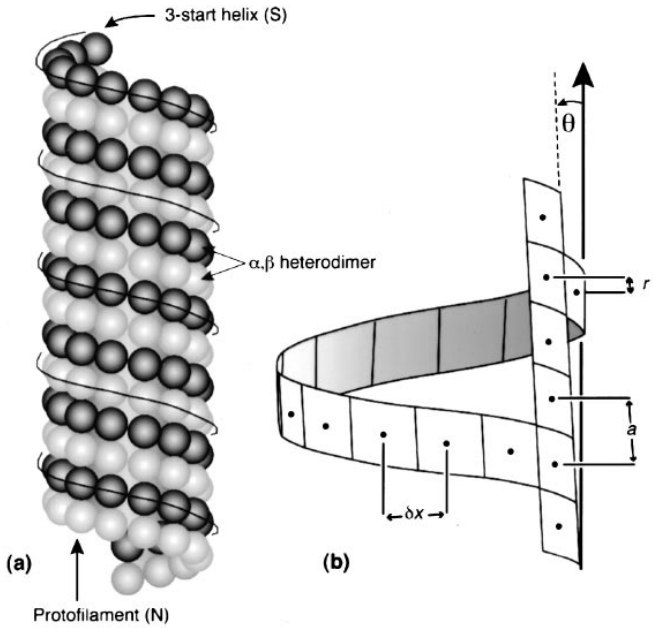

Fig. 1a, b Microtubule structure. **a** Schematic representation of a 13_3 microtubule. The α and β subunits of tubulin alternate along the protofilaments. The microtubule wall is made of 13 protofilaments running parallel to its longitudinal axis, and each protofilament is slightly shifted longitudinally with respect to its neighbor. This induces different helical families around the microtubule wall, one of which is the left-handed 3-start helix (S = 3) which follows neighboring subunits in adjacent protofilaments. The organization represented here corresponds to the "B-lattice" where homologue subunits alternate along the 3-start helix. **b** Parameters used to described the microtubule lattice. The differences between α and β subunits have been ignored, and only one protofilament and one 3-start helix are represented. The parameters a and δx represent the subunit spacing along and between protofilaments, respectively. The parameter r defines precisely the position of the lateral bonds between adjacent tubulin subunits along the S-start helix. The protofilament skew angle θ is observed in microtubules with a protofilament number different than 13 (here N = 14). The protofilament skew angle has been exaggerated for presentation purposes

ament bonds of factors that modify microtubule dynamic properties.

The microtubule lattice can be analyzed precisely using transmission electron microscopy. Earlier studies have shown that the tubulin molecule is aligned head-to-tail into protofilaments (Amos and Klug 1974), a variable number of which are juxtaposed to form the microtubule wall. Although it is widely considered that microtubules are made of 13 protofilaments, many exceptions are present in vitro as well as in vivo (see Chrétien and Wade 1991). Each protofilament is slightly shifted longitudinally with respect to its neighbor, giving rise to different helical families of the tubulin subunits around the microtubule wall. On a structural basis, the most important helical family is the left-handed 3-start helix because tubulin subunits interact laterally with their neighbors along this helical path (see Fig. 1). In a 13 protofilament microtubule, the position of the lateral bonds between neighboring subunits is such that every turn of the helix corresponds exactly to 13 subunits around the circumference of the microtubule, and to 3 subunits along the protofilaments. This condition is necessary to have the 13 protofilaments exactly parallel to the longitudinal axis of the microtubule. From this relationship, we can determine precisely the subunit rise r along this helix, which is also a measure of the position of the lateral bonds. Using a subunit length a of 40.5 Å (Hyman et al. 1995), we find $r = S \cdot a/N = 9.35$ Å, where S denotes the helix start number (S = 3) and N the protofilament number (N = 13). (Microtubules with N protofilaments and S-start helix will be noted N_S). Langford (1980) first noted that adding a protofilament to the basic 13_3 microtubule structure would break the helical symmetry if the protofilaments had to remain parallel to the microtubule axis (see also Wade et al. in the current issue). One possibility to correct this mismatch could be to decrease the helical rise by –0.67 Å to obtain a new value of $r = 8.68$ Å (N = 14 in the preceding formula). Although this corresponds to a very small modification of the inter-protofilament bonds, Langford noted that 14 protofilament microtubules assembled in vitro have skewed protofilaments, and proposed that the skew was necessary to accommodate the extra protofilament. However, detailed analysis was limited by the use of negative stain. The method of cryo-electron microscopy of vitrified specimens (cryo-EM, Dubochet et al. 1985) allowed Mandelkow et al. (1985) to visualize microtubules in a more native state. The protofilament skew was observed in 14 and 15 protofilament microtubules [1], and showed up as a moiré pattern repeating regularly along the microtubule images. These observations were extended to microtubules with from 11 to 17 protofilaments (Wade et al. 1990; Chrétien and Wade 1991), and a theoretical model which explains how microtubules accommodate different numbers of protofilaments was developed. The average experimental moiré period, which is directly related to the protofilament skew angle (see Theoretical background), was shown to be consistent with the theoretical prediction for the range of protofilament numbers observed. This analysis clearly demonstrated that microtubules accommodate different protofilament numbers by skewing their protofilaments, without modification of the lateral interactions between them. However, variability of the moiré period for a given type of microtubule was also noted, implying some flexibility in the microtubule lattice.

Here we evaluate several possible sources for the variability in the moiré patterns observed in 12_3 and 14_3 microtubules. We considered potential distortions of the microtubule during specimen preparation and variation in the parameters which describe the microtubule lattice. Our results reveal that small, systematic variation in the position of the lateral bonds between tubulin subunits in adjacent protofilaments can account for the observed variation in moiré patterns. This result provides an estimate of the flexibility of inter-protofilament bonds in microtubules assembled from pure tubulin in vitro. The methodology described

[1] 15 protofilament microtubules were wrongly assigned as 13 protofilament microtubules by the authors

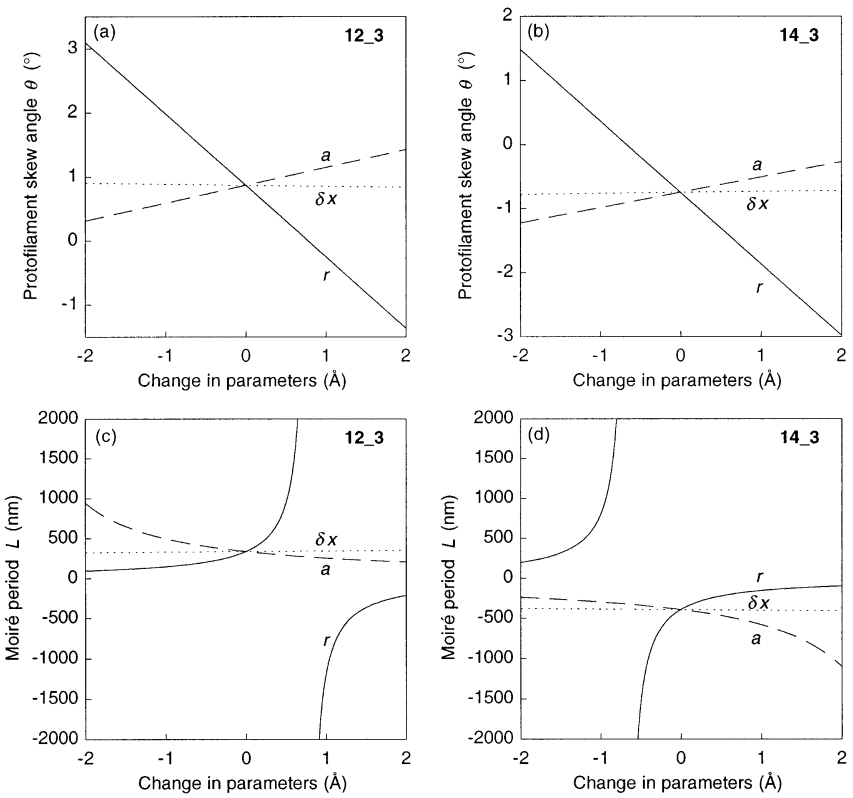

Fig. 2a–d Effect of small variations (±2 Å) in a, δx and r, on the protofilament skew angle θ and on the moiré period L for 12_3 and 14_3 microtubules. **a** Variations of θ for 12_3 microtubules. **b** Variations of θ for 14_3 microtubules. The point where the three curves intersect gives theoretical protofilament skew angles of +0.87° for 12_3 and –0.75° for 14_3 microtubules. **c** Variations of L for 12_3 microtubules. **d** Variations of L for 14_3 microtubules. The point where the three curves intersect gives theoretical moiré periods of +338 nm for 12_3 and –394 nm for 14_3 microtubules. These curves were calculated using Eqs. (1) and (3), with default values of a = 40.5 Å, δx = 51.3 Å, and r = 9.35 Å

here could be used to define the effects on the inter-protofilament interactions of agents which modify the dynamic properties of microtubules.

Experimental

The images used in this study were obtained from microtubules assembled in vitro from purified calf-brain tubulin. The protocols used to purify tubulin and to assemble microtubules have been given previously (Maaloom et al. 1994; Chrétien et al. 1995). Briefly, tubulin in 80 mM Pipes, a mM EGTA, 1 mM $MgCl_2$, pH 6.9 with KOH, and 1 mM GTP, was assembled into microtubules at 37 °C in the presence or absence of centrosomes. Nucleated assembly was performed at 6.5 µM, 13.0 µM and 19.5 µM and self-assembly at 44.0 µM. A 4 µl aliquot was pipetted at defined assembly times and deposited on a holey carbon-coated grid held by tweezers above a cup filled with liquid ethane. The humidity and the temperature of the sample were regulated using an environmental device (Chrétien et al. 1992). The aliquot was blotted using a filter paper to form a thin film spanning the holes of the carbon membrane and was rapidly plunged into liquid ethane at –190 °C. Electron microscope images of the microtubules were taken and the negatives were further enlarged for analysis. Some negatives were digitized and the tubulin dimensions were determined using computer image analysis. The magnification used to record each micrograph was calibrated using the position of the 1/40.5 Å layer line in the power spectrum of 13_3 microtubules. To calculate the moiré period, the distance between fuzzy regions in the moiré patterns of the microtubule was measured on prints. This distance corresponds to half the moiré period.

Theoretical background

Microtubules with 13 protofilaments and 3-start helices (noted 13_3) have their protofilaments parallel to the longitudinal axis of the microtubule. If one or more protofilaments is added or removed from the basic 13_3 microtubule structure, or if the helix-start number is changed, a mismatch is created at the junction between the 1st and Nth protofilament. This mismatch can be eliminated by skewing the protofilaments by an angle θ which can be predicted for any N_S microtubule using the following formula[2]:

$$\theta = \tan^{-1}\left(\frac{1}{\delta x}\left(\frac{\mathrm{S}\cdot a}{\mathrm{N}} - r\right)\right) \quad (1)$$

where r denotes the relative position of the lateral bonds between adjacent tubulin subunits along the S-start helix, δx the separation between protofilaments (subunit width),

[2] This formula has been modified with respect to previous publications where the sign of the protofilament skew angles was inverted (Chrétien and Wade 1991; Chrétien et al. 1996). In this paper, we use the normal convention which assigns a negative sign to a left-handed rotation, and a positive sign to a right handed rotation

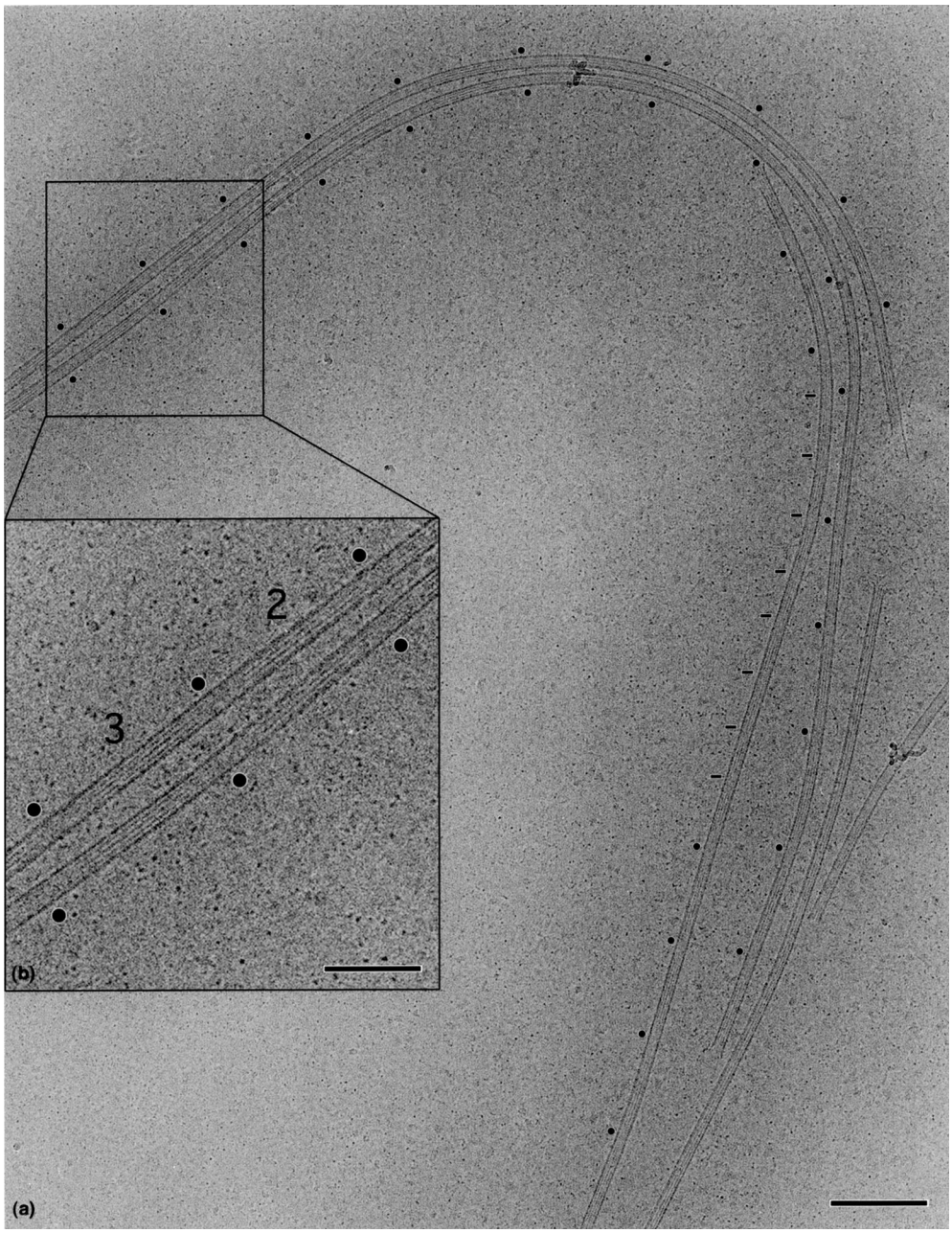

Fig. 3a, b Bent microtubules observed in vitreous ice. **a** Microtubules with from 13 to 15 protofilaments. The *dots* and the *bars* indicate fuzzy regions in the moiré patterns of 14 and 15 protofilament microtubules, respectively. One microtubule shows transitions from 14 to 15 protofilaments. Microtubules with 13 protofilaments (*bottom right*) do not show alternating moiré patterns. The *scale bar* is 200 nm. **b** Enlarged view of the boxed-in region in (**a**). The moiré pattern in 14 protofilament microtubules is composed of alternating regions of two and three central dark fringes separated by fuzzy regions (*dots*). The *scale bar* is 100 nm

and a the monomer spacing along protofilaments (subunit length), see Fig. 1b. For a given N_S microtubule, the protofilament skew angle θ will vary if r, δx, or a vary. Figures 2a and 2b show how θ will vary with changes of ±2 Å of each of these parameter for 12_3 and 14_3 microtubules, respectively. It can be seen that small changes in δx will have very little effect on the protofilament skew angle, whereas changes in a or r will have larger effects.

The protofilament skew generates a moiré pattern in the microtubules image whose period L is given by:

$$L = \frac{\delta x}{\sin(\theta)} \tag{2}$$

The sign of θ can be further determined by analyzing the diffraction pattern of the microtubule images, or by performing tilting experiments (Chrétien et al. 1996). The protofilament skew angle of microtubules is in general low, in the range –2° to +2°. It follows from Eq. (2) that small variations in the protofilament skew angle will induce large variations of the moiré period. Figures 2c and 2d show how the moiré period will vary with r, δx and a for 12_3 and 14_3 microtubules, respectively. Small changes in δx would not significantly affect the moiré period, whereas changes in a or r would have larger effects. In particular, an increase of +0.78 Å in r would straighten the protofilaments of 12_3 microtubules, while a decrease of –0.67 Å would have the same effect on 14_3 microtubules (see also Introduction).

Results

Microtubules were assembled at 37 °C from pure tubulin and prepared for cryo-EM after defined assembly times. Microtubules with from 10 to 16 protofilaments were observed, with variations depending on the tubulin concentration, the presence or absence of centrosomes, and the assembly time (details will be given in a following paper). Here, we will focus on the 12_3 and 14_3 microtubules which were the most abundant populations of microtubules with skewed protofilaments observed during this study.

We first asked whether the moiré period variations observed in vitrified microtubules could be due to artifacts induced during specimen preparation. Figure 3a shows microtubules bent during the formation of the thin layer of the suspension, and Fig. 3b is an enlarged view of the boxed-in region in (a). The protofilament skew in 14_3 microtubules shows up as a moiré pattern formed by alternating regions of – three central dark fringes – a fuzzy region – 2 central dark fringes – a fuzzy region – repeating along the microtubule image. The dark dots indicate fuzzy regions and thus, are spaced at half the moiré pattern repeat. The two 14_3 microtubules at the top of Fig. 3a show both straight and curved regions, but their moiré pattern repeat remain fairly constant. Figure 4 shows an analysis made on ~20 µm of straight (Fig. 4a) and highly curved (Fig. 4b) microtubules. The two distributions do not differ significantly (χ^2, $P > 0.05$), and show the same mean of –222 nm. This analysis clearly shows that bending does not affect the protofilament skew angle of microtubules. Conversely, large variations of the moiré period could be observed in straight microtubules. Figure 5 shows cryo-EM images of relatively straight 14_3 microtubules. Figures 5a and 5a′ correspond to the same microtubule which has been split into two parts, the bottom of Fig. 5a being continuous with the top of Fig. 5a′. Figure 5b is another microtubule observed on the same specimen grid. The spacing between fuzzy regions increases from ~100 nm at the top of Fig. 5a to ~260 nm at the bottom of Fig. 5a′, and is ~400 to ~500 nm for the microtubule in Fig. 5b. Another potential artifact which could have modified the moiré period is flattening of the microtubules in the thin ice layer. Figure 6a–e shows profiles corresponding to two fringes regions of the microtubule segments labeled 1 to 5 in Fig. 5, and Fig. 6f is an overlay of the 5 profiles. It can be seen that the microtubule width remains constant, excluding flattening as a potential source of image distortion. In the following, we will consider possible changes of the tubulin subunit dimensions and of their lateral interactions between neighboring protofilaments.

Table 1 gives the local moiré period corresponding to the microtubule segments 1 to 5 in Fig. 5. A theoretical value of $L = -384$ nm can be calculated using Eqs. (1) and (2) for 14_3 microtubules. Deviations from this theoretical value could be due to variations in the subunit dimensions, δx and a, or of the relative position of the lateral bonds between tubulin subunits in adjacent profilaments r

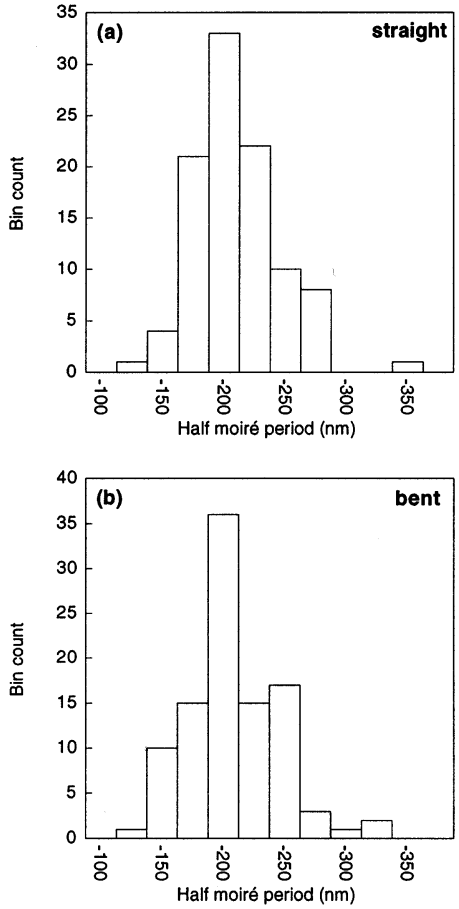

Fig. 4a, b Comparison between straight and bent microtubules. **a** Distance between fuzzy regions in straight 14_3 microtubules. **b** Distance between fuzzy regions in bent 14_3 microtubules. Microtubules with a high radius of curvature (~1 µm), and relatively straight microtubules present on the same negative were selected for the measurements. When feasible, the measurements were performed on the same microtubule showing both straight and curved regions, such as those presented in Fig. 3. 100 measurements were performed for each type of microtubule, and the data were binned at 25 nm intervals. Mean values of –222 ± 36 nm and –222 ± 38 nm were found for the distributions in (**a**) and (**b**), respectively (± represent the standard deviation of the distributions)

(see Fig. 2). The values expected for these parameters can be derived from Eqs. (1) and (2) (see Table 1):

$$\delta x = \sqrt{\frac{1}{2}\left(\frac{S \cdot a}{N} - r\right)^2 \left(-1 + \sqrt{1 + \left(\frac{2 \cdot L \cdot N}{S \cdot a - N \cdot r}\right)^2}\right)} \tag{3}$$

$$a = \frac{N}{S}\left(\frac{\delta x^2}{L\sqrt{1 - \left(\frac{\delta x}{L}\right)^2}} + r\right) \tag{4}$$

$$r = \frac{S \cdot a}{N} - \frac{\delta x^2}{L\sqrt{1 - \left(\frac{\delta x}{L}\right)^2}} \tag{5}$$

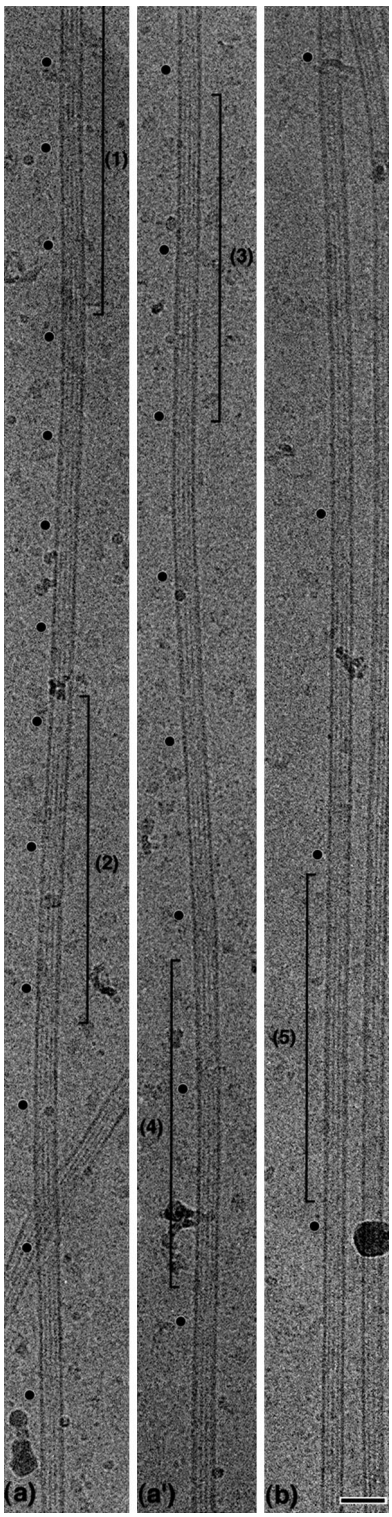

Fig. 5 a, b Variation of the moiré period in straight microtubules. **a**, **a′** 14_3 microtubule. The *bottom* of (**a**) is continuous with the *top* of (**a′**). **b** 14_3 microtubule showing a long moiré period. The microtubule segments labeled 1 to 5 have been analyzed to find the origin of the variations in moiré period. The *scale bar* is 50 nm

Table 1 Analysis of microtubule images

Microtubule segment		1	2	3	4	5
L	nm	–207	–326	–391	–446	–836
Expected parameters						
δx	(Å)	37.2	46.6	51.1	54.6	74.7
a	(Å)	37.7	39.8	40.5	40.9	42.1
r	(Å)	10.0	9.5	9.4	9.3	9.0
Measured parameters						
w	(Å)	266	271	270	273	268
δx	(Å)	50.5	51.6	51.4	52.1	50.9
a'	(Å)	40.5	40.5	40.1	40.5	40.5
θ	(°)	–1.40	–0.91	–0.75	–0.67	–0.35
α	(°)	–76.0	–75.2	–75.8	–75.8	–75.8
a	(Å)	40.7	40.7	40.2	40.6	40.6
r	(Å)	10.0	9.5	9.3	9.3	9.0
Measured changes in parameters						
$\Delta\delta x$	(Å)	0.0	+1.1	+0.9	+1.6	+0.5
Δa	(Å)	+0.2	+0.2	–0.3	+0.1	+0.1
Δr	(Å)	+0.6	+0.2	0.0	0.0	–0.3

L corresponds to the moiré period of the 5 microtubule segments in Fig. 5. The negative sign of *L* indicates that the protofilaments are left-handed[2]. The expected values of δx, *a* and *r* that could give rise to these moiré periods were calculated using Eqs. (3), (4) and (5), respectively, using default values of δx = 51.3 Å, *a* = 40.5 Å and *r* = 9.35 Å in the right-hand terms of the equations. The width *w* of the microtubule segments was measured on the image profiles (Fig. 6), and the subunit width δx was interpolated from the curve in Fig. 7. The parameter a' is the actual position along the meridian of the "1/40.5 Å" layer line in the power spectrum of the microtubule images (Fig. 8). The protofilament skew angle θ was calculated using Eq. (2) and the angle α was measured directly on the power spectrum of the microtubule images (Fig. 8). The subunit length *a* and the position of the interprotofilament bonds *r* were calculated using Eqs.(7) and (5), respectively. The measured changes in parameters correspond to the difference between the measured and the default values given above

The separation between protofilaments can be determined from the microtubule image width. The width of the profiles in Fig. 6 a–e was measured arbitrarily at 0.25 of their maximum intensity (*w* in Table 1). The protofilament separation can be deduced from these values providing that the increment in image width versus protofilament number is known (Chrétien and Wade 1991). Figure 7 shows this curve for microtubules with from 12 to 16 protofilaments observed during this study. To a good approximation[3], the increase in microtubule width versus protofilament number follows a straight line whose slope *s* is related to the protofilament separation by $s = \delta x/\pi$. From the linear fit of the data in Fig. 7, we find δx = 51.3 Å. The separation between protofilaments can be interpolated from this curve for any microtubule using:

$$\delta x = \frac{\pi}{\mathrm{N}}\left(w - 41.0\right) \qquad (6)$$

[3] In theory, the diameter of the microtubule should increase with the protofilament skew angle by a factor 1/cos (θ). For low protofilament skew angles, this effect can be neglected

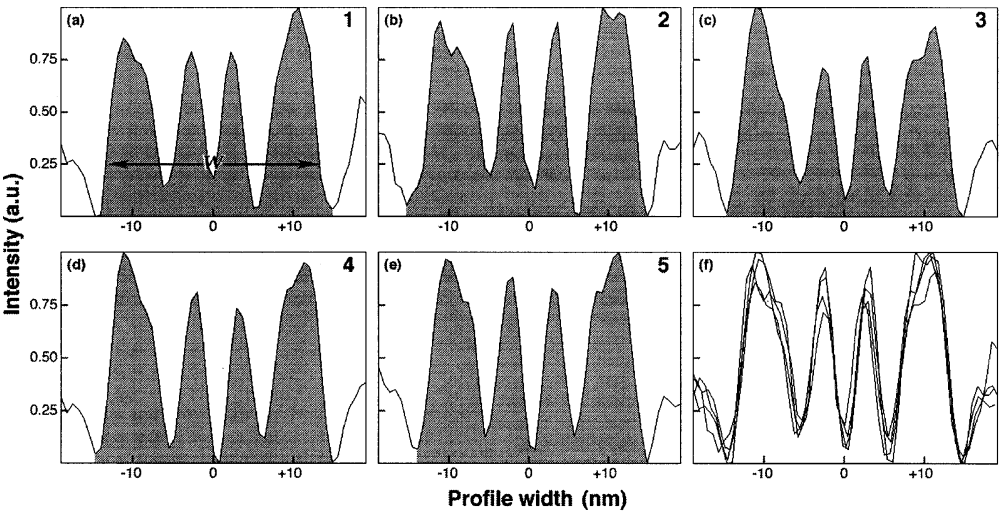

Fig. 6 a–f Determination of microtubule width. **a–e** Profiles of the microtubule segments labeled 1–5 in Fig. 5. These profiles were calculated by extracting a small region corresponding to two central dark fringes, and by projecting it along the longitudinal axis of the microtubule. The area of the profile corresponding to the microtubule has been shaded for clarity. The strong negative peaks surrounding the profiles are an effect of the contrast transfer function of the electron microscope. Microtubule width was calculated at 0.25 of the maximum intensity of the profiles (*w* in **a**). **f** Overlay of the 5 profiles

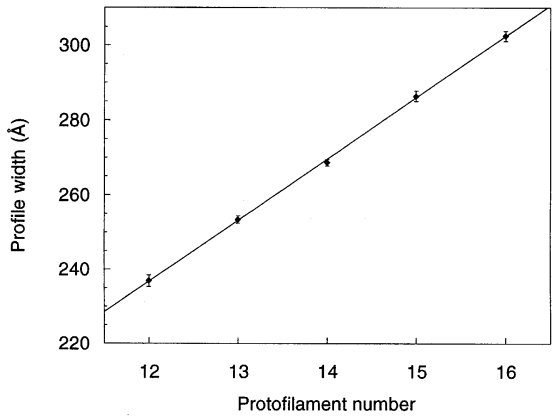

Fig. 7 Increase in microtubule width versus protofilament number. This curve was obtained using 91 microtubules with protofilament numbers ranging from 12 to 16. The *bars* represent standard error of the mean. Linear regression analysis gave $w = 16.32\ N + 41.0$, with $R = 0.96$

The values of δx calculated for the 5 microtubule segments in Fig. 5 are given in Table 1. It can be seen that these values are very close to the average value of 51.3 Å, which excludes variations in subunit width as a potential source of moiré period variation.

The monomer spacing along protofilaments can be accurately determined from the calculated power spectrum of the microtubule images. Figure 8a shows the power spectrum of a 13_3 microtubule present in the image. It is characterized by a strong layer line on the equator which includes information coming from the overall cylindrical structure of the microtubule and from its 13 protofilaments. The monomer repeat along the protofilaments gives rise to a layer line (*arrow*) spaced at 1/40.5 Å, and which can be used as an internal standard to calibrate the magnification of the image. Figures 8b–f show the power spectra of the 5 microtubule segments in Fig. 5. The skew of the protofilaments originates an additional layer line slightly offset from the equator, and whose position along the meridian will vary with the protofilament skew angle. Similarly, the protofilament skew modifies the position of the "1/40.5Å" layer line which will be shifted towards the equator for microtubules with right-hand protofilaments, and away from the equator for microtubules with left-handed protofilaments (Chrétien et al. 1996; Metoz et al. 1997). The amount of shift along the meridian will depend on the protofilament skew angle θ, and on the angle α between the equator and a line joining the center of the transform to the first peak of the layer line (see Fig. 8b). To a good approximation, the real spacing a along protofilaments can be estimated using:

$$a = a' \left(\frac{\cos(\theta) \cdot \tan(\alpha)}{\tan(\alpha) - \sin(\theta)} \right) \tag{7}$$

where a' is the actual position of the layer line along the meridian. The value of α can be directly measured on the power spectrum, and θ can be calculated using Eq. (2), since both the moiré period L and the protofilament separation δx are known. The calculated values of a are given in Table 1 for the 5 microtubule segments of Fig. 5. The *arrowheads* in Figs. 8b–f indicate the positions expected for the 1/40.5 Å layer lines if changes in the subunit spacing along protofilaments had been responsible for the moiré period variations.

The experimental value of r can be calculated using Eq. (5) if all the other parameters are known. Table 1 gives the values of r deduced from this analysis. Although these values are close to the theoretical value of 9.35 Å, it should be remembered that small changes in r can induce large variations in the moiré period L (see Fig. 2). The last three rows of Table 1 give the difference between the measured and the theoretical values of δx, a, and r for the 5 microtubule segments in Fig. 5. It can be seen that variations in the tubulin subunit dimensions (δx and a) cannot be responsible for the observed variations in the moiré pattern length. However, the values calculated for the relative position of the inter-protofilament bonds r are in good agreement with the expected values, indicating that small variations of this parameter (between –0.3 and +0.6 Å for the microtubules in Fig. 5) are the most likely sources of moiré period variations.

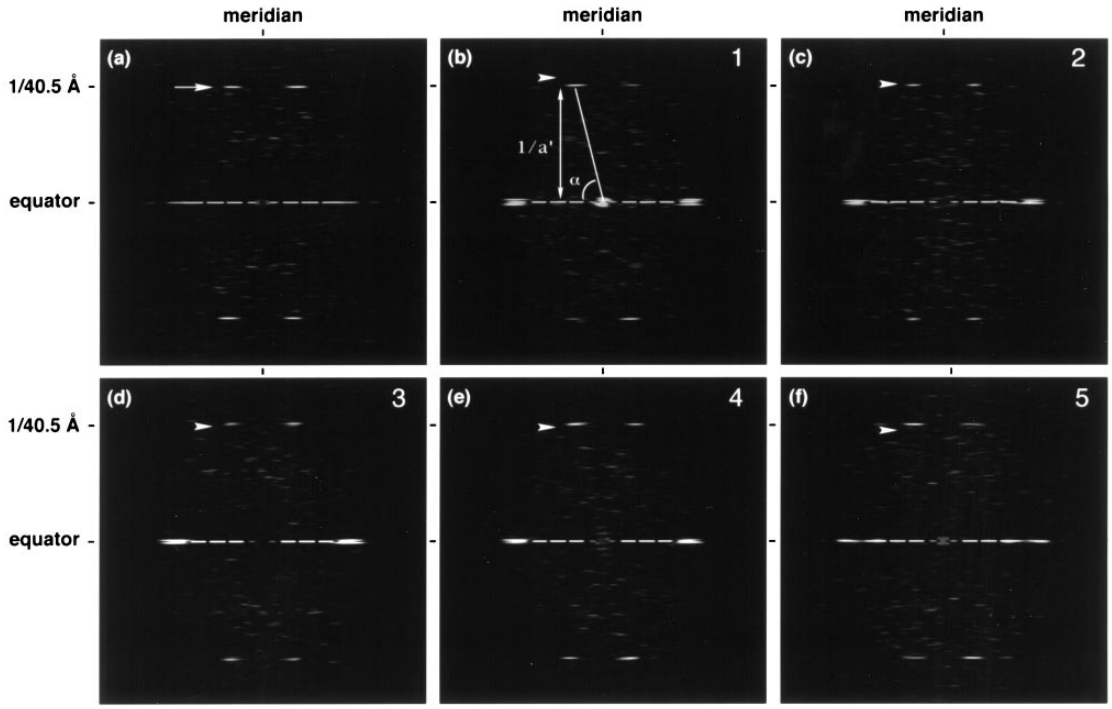

Fig. 8a–f Determination of the subunit spacing along protofilaments. **a** Power spectrum of a 13_3 microtubule. The *arrow* indicates the position of the 1/40.5 Å layer line. **b–f** Power spectra of the microtubule segments 1–5 in Fig. 5. The distance $1/a'$ is the actual position of the layer line along the meridian. The angle α defines the angle made between the equator and a line joining the center of the transform to the main peak of the layer line. The arrowheads indicate the positions expected for the layer line, if the subunit and the moiré pattern lengths of the corresponding microtubule segments were related

Table 2 Summary analysis

Microtubule type		12_3		14_3	
		mean	range	mean	range
δx	(Å)	51.5 ± 0.5	48.4 ~ 56.5	51.2 ± 0.2	49.1 ~ 53.2
a	(Å)	40.5 ± 0.1	39.8 ~ 40.8	40.5 ± 0.1	40.0 ~ 40.7
$1/2\ L$	(nm)	177 ± 26	104 ~ 426	–222 ± 36	–508 ~ –84
Δr	(Å)	0.0 ± 0.1	–0.5 ~ +0.5	–0.1 ± 0.1	–0.4 ~ +0.9

The values of δx and a were determined on 20 microtubules of each type selected randomly from the images used to calculate the distributions in Fig. 9a, b (± indicates the standard error of the mean). The average distance between fuzzy regions ($1/2\ L$) and the average variation of the inter-protofilament bonds (Δr) were derived from the distributions in Fig. 9. They are given ± the standard deviation of the distributions. The range indicates the minimum and maximum values measured

Figure 9 shows the results of an extensive analysis performed on 359 12_3 and 924 14_3 microtubule segments. The distributions are peaked around 177 nm for the 12_3 microtubules (Fig. 9a) and –222 nm for the 14_3 microtubules (Fig. 9b), and show variations in the range +104 to +426 nm and –508 to –84 nm, respectively. 20 microtubules of each type selected randomly from these two distributions were analyzed in more detail (see Table 2). As for the 5 microtubule segments in Fig. 5, we found slight variations in both the subunit width and length for each type of microtubule. It is likely that the variations in subunit width reflect essentially the various amounts of noise included in the measurement of the image width and the effect of the contrast transfer function (CTF) of the electron microscope. This effect shows up as light fringes surrounding the microtubule images (see Figs. 3 and 5), and as deep valleys below the background level surrounding the image profiles (see Fig. 6). The effect of the CTF will vary with the image defocus and thus, may add variability in our measurements of microtubule width from one image to another. By contrast, the position of the layer line in the power spectrum of the microtubule images is not affected by the CTF (only its intensity). In addition, the step size used to scan the images was such that a variation ~0.3 Å in subunit size corresponded to a change of 1 pixel in layer line position. Thus, the observed variations of –0.7 Å to +0.3 Å of the tubulin repeat along protofilaments are more likely to reflect real variations in subunit length. The same degree of variability was found in regular 13_3 microtubules (data not shown). However, neither the variations in subunit length nor in subunit width are sufficiently large to explain the broad range of moiré periods observed in the microtubules images. Thus, as demonstrated in the previous analysis, these variations must be accounted for by small variations of the position of the inter-protofilament bonds. We translated the moiré pattern distributions in Figs. 9a and 9b into variations of the position of the inter-protofilament bonds for the 12_3 (Fig. 9c) and 14_3 (Fig. 9d) microtubules, using Eq. (5) and the average values of δx and a measured for each type of microtubule. The two distributions are peaked around 0.0 Å and –0.1 Å for the 12_3 and 14_3 microtubules, respectively (see also

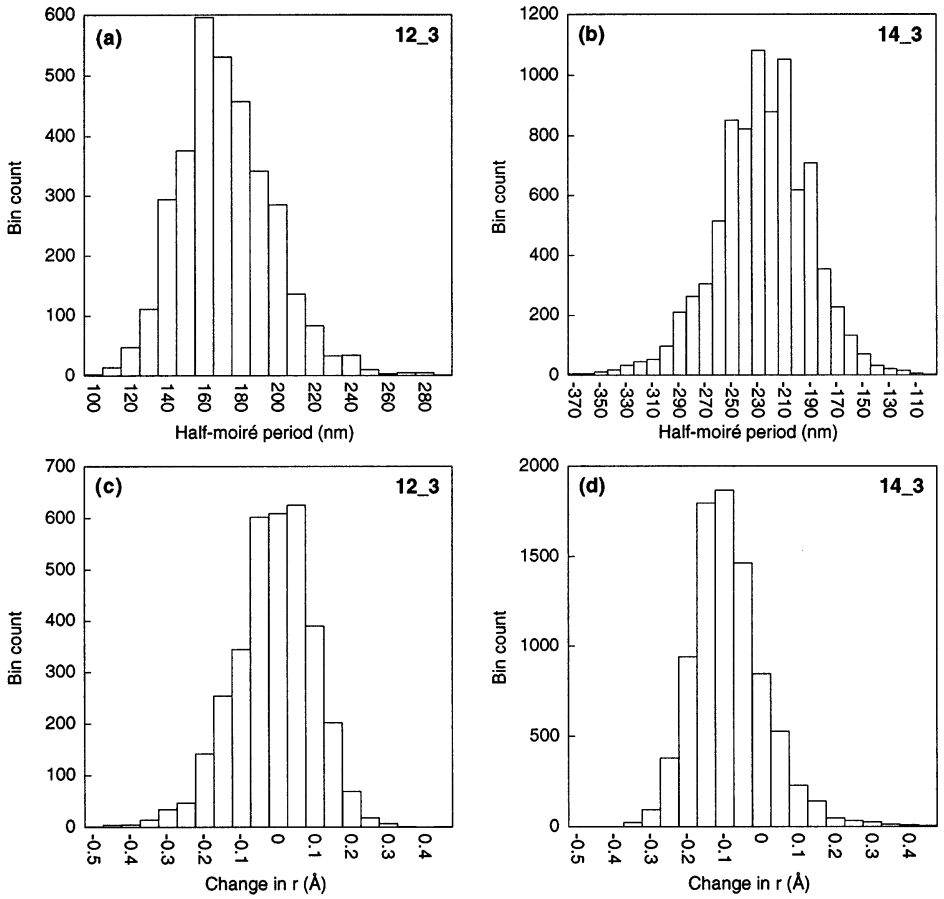

Fig. 9a–d Variations of the inter-protofilament bonds in 12_3 and 14_3 microtubules. **a** Half-moiré period in 12_3 microtubules. A total of 359 microtubules was analyzed, corresponding to 3368 measurements of the distance between fuzzy regions. **b** Half-moiré period in 14_3 microtubules. A total of 924 microtubules was analyzed, corresponding to 8460 measurements of the distance between fuzzy regions. The data were binned at 10 nm interval. **c** Variations of the inter-protofilament bonds in 12_3 microtubules. **d** Variations of the inter-protofilament bonds in 14_3 microtubules. The difference between the measured and the theoretical values of *r* were calculated for each 1/2 moiré period measurement, using Eq. (5), and the average values of δx and *a* calculated for each type of microtubule (Table 2). The data were binned at 0.05 Å interval. These distributions extend slightly beyond the limits indicated in the figures. The full ranges are given in Table 2

Table 2). This clearly shows that the main mechanism used by microtubules to accommodate different protofilament numbers is to skew their protofilaments, without noticeably changing their inter-protofilament interactions (Wade et al. 1990; Chrétien and Wade 1991). In addition, the large variations in moiré period translate into slight variations of the inter-protofilament interactions in the range –0.5 Å to +0.9 Å. These variations are sufficiently small to be interpreted as reflecting the flexibility of the inter-protofilament bonds in microtubules assembled from pure tubulin.

Discussion

In this study, we have used the variability present in the moiré patterns of microtubules observed by cryo-EM to determine the precision by which tubulin subunits interact laterally between adjacent protofilaments. We found small variations, in the range –0.5 Å to +0.9 Å, of the relative positions of these bonds. Before discussing the implications of these results, we would like to give some comments about the methods used to obtain these fine measurements.

It may appear paradoxical that, working with images at a resolution of ~40 Å, we can obtain a precision which is on the order of the inter-atomic distance. First, it should be realized that these values are not obtained on individual molecules, but are local averages over several tens of nm corresponding to many subunits. The average distance between fuzzy regions in a 14 protofilament microtubule is about 200 nm, which corresponds to ~700 subunits (or ~350 tubulin molecules). Similarly, a power spectrum used to calculate the subunit repeat along protofilaments is obtained on a typical length of ~360 nm, corresponding to ~1250 subunits. Second, this precision in the measurements is due to the combination of the high magnification power of the electron microscope with the fact that the protofilament skew angle is in general very low. The length of the moiré pattern is inversely proportional to the sine of the protofilament skew angle (Eq. (2)) and thus, tends towards infinity when this angle approaches zero. It follows that any change in the microtubule lattice organization that affects the protofilament skew angle will show up as large changes in the moiré period (see Fig. 2). This sensitivity of the moiré period has been used in two preceding studies where small changes in the subunit length were correlated with substantial changes in the moiré period (Hyman et al. 1995; Arnal and Wade 1995).

The variations that we measured are only meaningful if they reflect the state in which the microtubules were in solution before preparing the sample for cryo-EM. The time required to plunge the specimen into liquid ethane is on the order of a few tens of msec, and the cooling time is probably less than a msec (Fuller et al. 1995). Thus, large

conformational changes of the tubulin molecules, due for example to cooling, are very unlikely. Other artifacts that could modify the fine structure of the microtubules are bending and flattening. A detailed comparison between the moiré period of straight and highly bent microtubules did not reveal a significant difference between the two populations. This is an important observation, since it clearly indicates that bending does not modify the relative position of the inter-protofilament bonds. Thus, the flexibility of the microtubules must be related to another property of the microtubule lattice, the most likely being stretching and compressing of the tubulin subunits along the protofilaments. The highest radii of curvature observed were on the order of 1 µm, which corresponds to a difference in length of ~2% between the two sides of the microtubule. If both stretching and compression occur, this represents a change of ~0.4 Å in subunit length, which is on the order of the variations recorded for the subunit spacing along protofilaments (see Tables 1 and 2). We also demonstrated that flattening was not involved in the moiré period variation. Thus, the origin of these variations must reflect some flexibility in the tubulin subunits or of their interactions in the microtubule lattice.

Based on theoretical considerations, variations in subunit width were very unlikely, since changes of several tenths of Å would have been required to account for the range of moiré periods observed (see Table 1). Such large variations in subunit width would have induced large variations in the microtubule diameter, which would have been easily detected by eye on the negatives, and image analysis clearly confirmed that variations in subunit width were not involved. Another source of moiré period variation could have been small variations of a few Å of the subunit spacing along protofilaments. In a preceding study (Hyman et al. 1995), it was shown that an increase of ~1.5 Å in subunit length was correlated with a shift of the average moiré period of ~170 nm in 14_3 microtubules. However, the variations in subunit length that we measured were only of a few tenths of Å, and were not correlated with variations in the moiré period. It follows that the more likely source of moiré period variation are small differences of the position of the lateral bonds between neighboring subunits in adjacent protofilaments. Theoretical calculations show that the moiré period is highly sensitive to small changes in this parameter (Fig. 2). Variations in the moiré period can be observed in any type of microtubule, and in particular in 13_3 microtubules where various amounts of protofilament skew can be observed (unpublished observations). Unfortunately, these microtubules cannot be used for image analysis because their moiré patterns are usually very long, and no accurate measurement of the moiré period can be performed. Microtubules with 12 and 14 protofilaments are more suited because their moiré period is comprised between ~0.2 µm and ~1.0 µm, lengths which can be easily recorded on negatives by electron microscopy. Our analysis shows that these large variations in the moiré period translate into small variations, of a few tenths of angström, of the position of the lateral bonds between neighboring subunits in adjacent protofilaments.

The variation in the parameters of the microtubule lattice which are documented here give rise to a different description of a microtubule than one which focuses on local interactions. These variations are almost imperceptibly small for a single subunit. Indeed, variations of a similar size are attributed to the breathing motions of proteins. The special characteristic of these distortions is that they are concerted, that a systematic small variation is present in all the subunits of a microtubule. Hence the variation in moiré pattern reflects the presence of local distortions coordinated over a long range which may correspond to very small amounts of energy. Thus, although it is not possible to give a detailed explanation for these variations at the molecular level, they are sufficiently small to be quite comparable to distortions caused by thermal bending of microtubules. If, indeed, the energy associated with the variations in the microtubule lattice documented here are of order of kT, then by the unbeatable logic of thermal fluctuations, they may be just that. To test this hypothesis, it may be worth studying the effect of temperature on the variability of the moiré period. The prospects for observable effects are not good, though, due to the limited range of temperatures in which microtubules can be studied.

One important conclusion that can be drawn from this and previous studies (Chrétien and Wade 1991; Wade et al. 1990) is that the inter-protofilament interactions are very precisely maintained in microtubules, even though GTP-hydrolysis occurred. This observation may relate to the fact that GDP-protofilaments are highly constrained in a straight conformation in microtubules (Melki et al. 1989, see also Jánosi et al. in the current issue). Upon microtubule depolymerization, the protofilaments peel off radially from the microtubule wall and adopt a curved conformation (~20 nm in radius of curvature), which presumably corresponds to their minimal energy configuration. Thus, deformation of the inter-protofilament bonds in microtubules may require so much energy that only small fluctuations are allowed. Interestingly, Hyman et al. (1995) measured larger variations of the moiré period in 14_3 GMPCPP-microtubules (640±97 nm) compared to 14_3 GDP-microtubules (466±38 nm). This result is consistent with the observation that GMPCPP-protofilaments are straighter, and hence less constrained, than GDP-protofilaments in microtubules (Müller-Reichert et al. 1998). Our results also provide some useful information concerning the forces which are at play in the microtubule lattice. The mechanism used by microtubules to accommodate different numbers of protofilaments indicates that it is energetically more favorable for a microtubule to skew its protofilaments than to modify the lateral bonds that hold them together, even by a fraction of Å (see Introduction). In addition, bending has no measurable effect on the inter-protofilament bonds, implying that deformation of the subunit molecule is the more likely mechanism used by the microtubule to accommodate bending (see above). This indicates that these bonds are relatively stiff, a condition required to provide high rigidity to the microtubule lattice (Gittes et al. 1993; Felgner et al. 1996).

In conclusion, analysis of the moiré pattern of vitrified microtubules observed by cryo-EM appears to be a very sensitive method to detect small modifications of the microtubule lattice. We are confident that the methodology developed in this study can be used to investigate the effects of factors that modify the dynamic and mechanical properties of microtubules. This include GTP-analogues, MAPs, drugs, and also changes in the physico-chemical environment of the microtubules (temperature, pH, Ca^{2+}, Mg^{2+}, Glycerol, …).

References

Amos LA, Klug A (1974) Arrangement of subunits in flagellar microtubules. J Cell Sci 14:523–549

Arnal I, Wade RH (1995) How does taxol stabilize microtubules? Curr Biol 5:900–908

Avila J (1990) Microtubule proteins, CRC Press, Boca Raton, Florida

Caplow M (1992) Microtubule dynamics. Curr Op Cell Biol 4:58–65

Chrétien D, Fuller SD, Karsenti E (1995) Structure of microtubule ends: two-dimensional sheets close into tubes at variable rates. J Cell Biol 129:1311–1328

Chrétien D, Kenney JM, Fuller SD, Wade RH (1996) Determination of microtubule polarity by cryo-electron microscopy. Structure 4:1031–1040

Chrétien D, Metoz F, Verde F, Karsenti E, Wade RH (1992) Lattice defects in microtubules: Protofilament numbers vary within individual microtubules. J Cell Biol 117:1031–1040

Chrétien D, Wade RH (1991) New data on the microtubule surface lattice. Biol Cell 107:161–174

Dubochet J, Adrian M, Lepault J, McDowall AW (1985) Cryo-electron microscopy of vitrified biological specimens. TIBS 10:143–146

Erickson HP, O'Brien ET (1992) Microtubule dynamic instability and GTP hydrolysis. Ann Rev Biophys Biomol Struct 21:145–166

Felgner H, Frank R, Schliwa M (1996) Flexural rigidity of microtubules measured with the use of optical tweezers. J Cell Sci 109:509–516

Fuller SD, Berriman JA, Butcher SJ, Gowen BE (1995) Low pH induces swiveling of the glycoprotein heterodimers in the Semliki Forest Virus spike complex. Cell 81:715–725

Gittes F, Mickey B, Nettleton J, Howard J (1993) Flexural rigidity of microtubules and actin filaments measured from thermal fluctuations in shape. J Cell Biol 120:923–934

Hyams JS, Lloyd CS (1994) Microtubules, Wiley-Liss, New York

Hyman AA, Chrétien D, Arnal I, Wade RH (1995) Structural changes accompanying GTP hydrolysis in microtubules: information from a slowly hydrolyzable analogue guanylyl(α-β)methylenediphosphonate. J Cell Biol 128:117–125

Hyman AA, Karsenti E (1996) Morphogenetic properties of microtubules and mitotic spindle assembly. Cell 84:401–410

Langford GM (1980) Arrangement of subunits in microtubules with 14 protofilaments. J Cell Biol 87:521–526

Maaloum M, Chrétien D, Karsenti E, Hörber JKH (1994) Approaching microtubule structure with the scanning tunneling microscope. J Cell Sci 107:3127–3131

Mandelkow E-M, Mandelkow E (1985) Unstained microtubules studied by cryo-electron microscopy: substructure, supertwist and disassembly. J Mol Biol 181:123–135

Mitchison T, Kirschner M (1984) Dynamic instability of microtubule growth. Nature 312:237–242

Metoz F, Arnal I, Wade RH (1997) Tomography without tilt: Three-dimensional imaging of microtubule/motor complexes. J Struct Biol 118:159–168

Müller-Reichert T, Chrétien D, Severin F, Hyman AA (1998) Structural changes at microtubule ends accompanying GTP-hydrolysis: information from a slowly hydrolyzable analogue of GTP, guanylyl(α,β)methylenediphosphonate. Proc Natl Acad Sci USA 95:3661–3666

Wade RH, Chrétien D, Job D (1990) Characterization of microtubule protofilament numbers: how does the surface lattice accommodate? J Mol Biol 212:775–768

Walker RA, O'Brien ET, Prier NK, Soboeiro MF, Voter WA, Herickson HP, Salmon ED (1988) Dynamic instability of individual microtubules analyzed by video light microscopy: Rate constants and transition frequencies. J Cell Biol 107:1437–1448